

Site-Specific Analysis of Protein Hydration Based on Unnatural Amino Acid Fluorescence

Mariana Amaro,[†] Jan Brezovský,^{‡,§} Silvia Kováčová,^{||,§} Jan Sýkora,[†] David Bednář,^{‡,§} Václav Němec,^{||,§} Veronika Lišková,[‡] Nagendra Prasad Kurumbang,^{‡,#} Koen Beerens,[‡] Radka Chaloupková,[‡] Kamil Paruch,^{*,||,§} Martin Hof,^{*,†} and Jiří Damborský^{*,‡,§}

[†]J. Heyrovsky Institute of Physical Chemistry of the ASCR, v. v. i., Academy of Sciences of the Czech Republic, Dolejskova 3, 182 23 Prague 8, Czech Republic

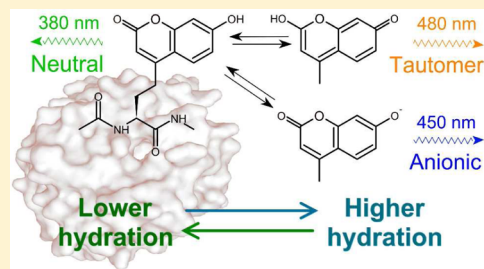
[‡]Loschmidt Laboratories, Department of Experimental Biology and Research Centre for Toxic Compounds in the Environment RECETOX, Faculty of Science, Masaryk University, Kamenice 5/A13, 625 00 Brno, Czech Republic

^{||}Department of Chemistry, Faculty of Science, Masaryk University, Kamenice 5/A13, 625 00 Brno, Czech Republic

[§]International Clinical Research Center, St. Anne's University Hospital Brno, Pekarska 53, 656 91 Brno, Czech Republic

Supporting Information

ABSTRACT: Hydration of proteins profoundly affects their functions. We describe a simple and general method for site-specific analysis of protein hydration based on the in vivo incorporation of fluorescent unnatural amino acids and their analysis by steady-state fluorescence spectroscopy. Using this method, we investigate the hydration of functionally important regions of dehalogenases. The experimental results are compared to findings from molecular dynamics simulations.



INTRODUCTION

Protein hydration is important in enzymatic catalysis¹ since it influences enzymes' kinetics² and enantioselectivity,³ protein folding,⁴ ligand-binding, and DNA–protein interactions.⁵ Hydration has been studied using X-ray absorption,⁶ NMR spectroscopy,⁷ neutron scattering,⁸ dielectric relaxation spectroscopy,⁹ two-dimensional infrared spectroscopy,¹⁰ and time-resolved fluorescence spectroscopy.¹¹ All these techniques provide valuable information on the arrangement of water molecules in the vicinity of specific protein moieties. However, they require costly and highly specialized instrumentation. Here we present a new technique for studying protein hydration using very basic laboratory instruments. Our approach is based on a recently developed method for the site-specific incorporation of unnatural amino acids (UAAs) into protein structures¹² and the analysis of their properties using steady-state fluorescence (SSF) spectroscopy. Additionally, we developed a more economical synthesis of L-(7-hydroxycoumarin-4-yl) ethylglycine, whose preparation had represented a bottleneck for its wider use in protein labeling. Furthermore, for the first time a quantitative analysis of the hydroxycoumarin fluorescence within a specific protein region is performed, followed by newly established data deconvolution that enables us to estimate the level of protein hydration. We demonstrate its effectiveness by characterizing the molecular environments of UAAs in the tunnel mouths of two haloalkane dehalogenases and comparing these experimental results to the output of

molecular dynamics (MD) simulations and previous reports.^{11,13}

RESULTS AND DISCUSSION

To deliver an UAA into a specific site encoded by a nonsense codon, the tRNA/aminoacyl-tRNA synthetase pair needs to be constructed. In this project we utilized the L-(7-hydroxycoumarin-4-yl) ethylglycine,¹⁴ which contains the fluorophore 7-hydroxy-4-methylcoumarin (7H4MC). The photophysics of 7H4MC is environment-sensitive.^{15,16} Three forms of 7H4MC, neutral, anionic, complexed, exist in equilibrium (Supporting Information Figure S1A), each with different excitation maxima.¹⁷ In addition, a tautomeric form can be created in the excited state via proton transfer between the spatially separated carbonyl and hydroxyl groups (Figure 1A, Supporting Information Figure S1B). Accordingly, the SSF spectra of all four excited state forms are shifted in respect to each other and thus their contributions to the overall signal can be separated. As the equilibria (both in the ground and excited states) are governed by the hydration state of the dye, information on the contributions of the corresponding microenvironments to the SSF spectra can be gained.

To demonstrate how the fluorescence of 7H4MC can provide information on the extent of hydration of its vicinity,

Received: July 26, 2014

Revised: February 14, 2015

Published: March 27, 2015

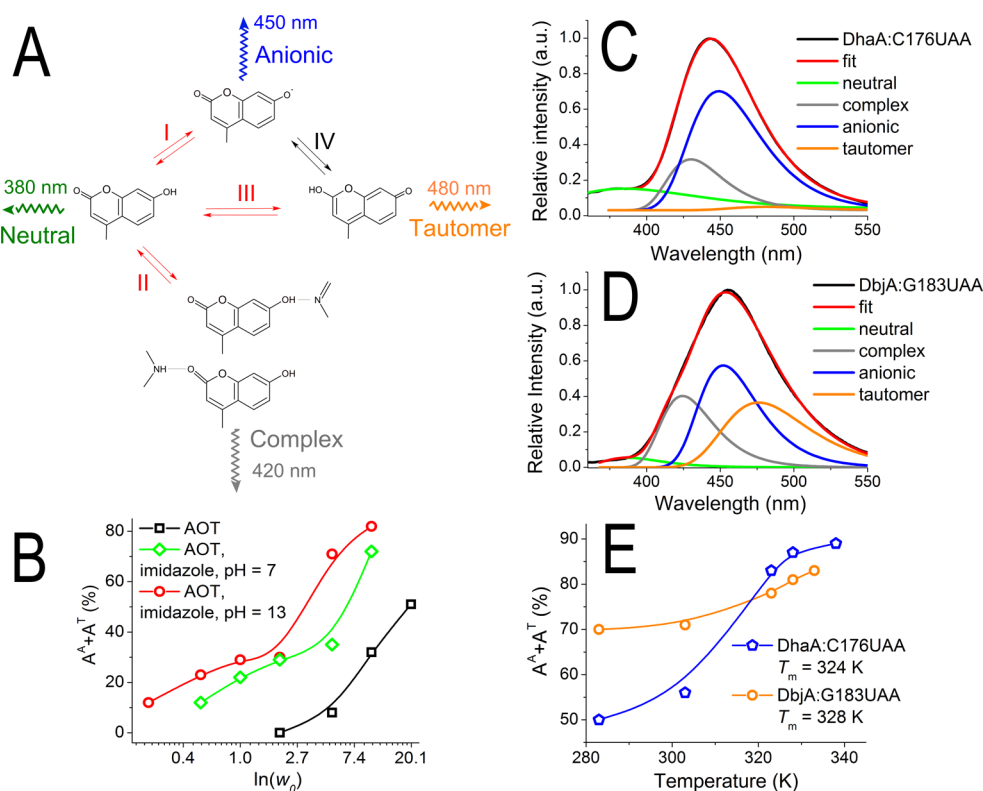


Figure 1. (A) General reaction scheme of 7H4MC in the excited state. Neutral, anionic and complexed (for instance with an adjacent amino group) forms of the fluorophore can exist and/or coexist. Proton transfer (reaction III) can additionally take place, creating a tautomeric form. This proton transfer has been shown to be promoted by the presence of “structured water”.¹⁵ In bulk water, anion formation (reaction I) prevails because the pK_a^* of the excited state is below 1.5.¹⁵ The numbers accompanying the rippled arrows correspond to the maximum of the emission spectra of each particular 7H4MC form. Red reaction arrows highlight the dominant pathways in the excited state. (B) Dependence of the hydration parameter on water content (w_0) in AOT micelles. The graph illustrates the increase in the magnitude of the fluorescence emission of the anionic and tautomer forms of 7H4MC (the sum of the decomposed spectrum areas emitted from the two forms) with the increasing amount of water added to the reverse AOT micelles (w_0). Imidazole was added in order to mimic $-\text{NH}^+$ and $-\text{NH}-$ functional groups present in the protein matrix, resulting in the formation of the complex form. The areas were gained by the decomposition of the steady-state emission spectra. (C and D) Emission spectra of UAA incorporated into DhaA:C176UAA and DbjA:G183UAA, respectively. The spectra were recorded at an excitation wavelength of 320 nm. The black curve represents the recorded emission spectrum; the green, gray, blue and orange curves represent its decomposition into the neutral, complexed, anionic and tautomeric components, respectively. The red curve stands for the result of the fit. (E) Hydration parameter upon thermal denaturation. The temperature dependence of the hydration parameter ($A^A + A^T$) was measured for both herein investigated proteins. T_m values given in the graph legend corresponds to the melting temperature, which is the temperature at which 50% of the protein becomes unfolded.

and specific interactions between the fluorophore and proton donors or acceptors, we decomposed its SSF spectra in docusate sodium (AOT) reverse micelles. At low water/surfactant molar ratios (w_0), water molecules associate strongly with the polar heads of the surfactant molecules, forming “structured water”. As w_0 increases, “bulk” water is created inside the reverse micelles. Studies on the photophysics of 7H4MC in reverse micelles^{15,16} have shown that in the absence of water ($w_0 \approx 0$) the dye fluoresces mainly from its neutral form. Stepwise addition of water causes an increasing contribution from the tautomeric form, with the anionic form also becoming important as w_0 increases further. The relative contributions of these particular 7H4MC forms can be determined by decomposing the corresponding SSF spectra (Supporting Information Figure S2). At $w_0 \approx 0$, only the neutral form (emission maximum wavelength ~ 380 nm) is present (Supporting Information Table S1 and Figure S2A). When w_0 rises above 10, the tautomer band (~ 480 nm) appears and gradually becomes more intense, indicating that the dye is surrounded by an increasing number of water molecules bound to the detergent’s polar headgroups. Note that even at very low w_0 values, the complexed form (~ 420 nm) can be detected if

proton donor or acceptor molecules are added to the AOT reverse micelles (Supporting Information Table S2). Further increases in the water content produce bulk water inside the reverse micelles, sharply increasing the contribution of the anionic band (~ 450 nm; Supporting Information Figure S2C). The anionic form is the dominant fluorescing species in bulk water. We utilized this sensitivity of 7H4MC photophysics and determined the sum of the contributions of the anionic and tautomer forms to the total emission spectrum (quantified by parameter $A^A + A^T$), whose formation is conditioned by the presence of water. Indeed, $A^A + A^T$ gradually rises with increasing water content w_0 for three different AOT systems (Figure 1B, Supporting Information Tables S1 and S2). This parameter can therefore be used as an indicator of the extent of hydration.

Prior to testing this approach in proteins, the synthesis of the UAA containing the 7H4MC fluorophore had to be optimized since gram quantities of UAA were required for the cultivation of recombinant *Escherichia coli*. We realized that the UAA is poorly soluble in the mobile phase previously used for HPLC purification (<400 mg/L).¹⁸ Therefore, we developed a new, significantly more economical protocol that avoids the use of

HPLC and utilizes ion exchange chromatography followed by precipitation. The fluorophore was inserted at specific locations within the sequences of two haloalkane dehalogenases DhaA:C176UAA and DbjA:G183UAA. The selected enzymes are functional variants derived from haloalkane dehalogenases DhaA from *Rhodococcus rhodochrous* NCIMB1306433¹⁹ and DbjA from *Bradyrhizobium japonicum* USDA110.²⁰ Circular dichroism analysis (Supporting Information Figure S3) and activity testing (Supporting Information Table S3) confirmed that introduction of the UAA did not disrupt the structure and the catalytic function of the enzymes. Although both enzymes catalyze nucleophilic substitution via the same mechanism their substrate specificity and enantioselectivity differ substantially.¹³ This is attributed to the different architectures of their active sites as well as access tunnels. The fluorescent UAA was inserted at the position 176 and 183 of DhaA and DbjA, respectively, to probe the hydration of their tunnels (Figure 2A) which are known to be important for enzyme function.^{3,13}

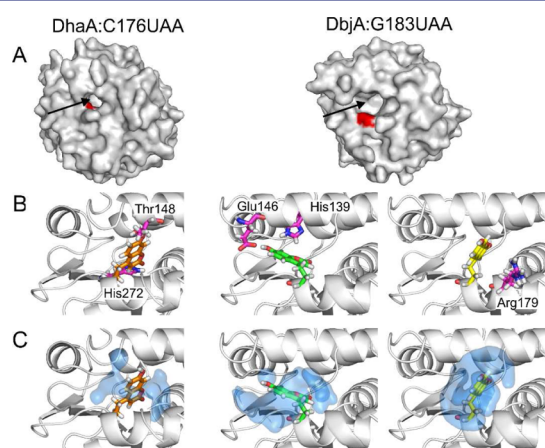


Figure 2. Local environment and hydration of the UAAs in DhaA:C176UAA and DbjA:G183UAA. (A) Positions of the UAAs (indicated by the red surface patches) and the tunnel mouths (indicated by black arrows) on the surface of the enzymes. (B) Local interactions of UAAs with hydrogen acceptors and amino groups (purple sticks). The buried (UAA_3) and exposed (UAA_4) conformations of the UAA in DbjA:G183UAA are indicated by green and yellow sticks, respectively. The conformation of the UAA in DhaA:C176UAA is indicated by the orange stick model. (C) Hydration of UAAs. The blue surface represents enzyme regions that are occupied by water molecules for at least 40% of the total simulation time.

Specifically, DhaA possesses a narrower tunnel and at the same time exhibits significantly lower enantioselectivity to β -bromoalkanes than DbjA.¹³ Recently, we have demonstrated that hydration and dynamics of the tunnel mouth are important determinants of DbjA enantioselectivity toward β -bromoalkanes.³ Thermodynamic analysis revealed that enantiodiscrimination of β -bromoalkanes by DbjA and DhaA is differently influenced by individual thermodynamic contributions—differential activation enthalpy ($\Delta_{R,S}\Delta H^\ddagger$) and entropy ($\Delta_{R,S}\Delta S^\ddagger$). While the resolution of 2-bromopentane by DbjA is driven almost equally by both enthalpic and entropic terms (where the entropic term represents 83% of the enthalpic term) the DhaA enantioselectivity is clearly dominated by enthalpy (Table 1). In both cases, the preferred (*R*)-enantiomer is favored by the enthalpy while the nonpreferred (*S*)-enantiomer is favored by the entropy. Interestingly, the enthalpic and the entropic

Table 1. Enantioselectivity and Its Thermodynamic Components for the Kinetic Resolution of 2-Bromopentane by Haloalkane Dehalogenases DhaA and DbjA^a

enzyme	<i>E</i> value 298 K	$\Delta_{R,S}\Delta H^\ddagger$ [kJ mol ⁻¹]	$T\Delta_{R,S}\Delta S^\ddagger$ ^{298K} [kJ mol ⁻¹]	$\Delta_{R,S}\Delta G^\ddagger$ ^{298K} [kJ mol ⁻¹]
DhaA	20	-15.37	-8.22	-7.15
DbjA ^b	132	-69.51	-57.78	-11.73

^a*E* value—enzyme enantioselectivity, $\Delta_{R,S}\Delta G^\ddagger$ —differential free energy of activation between (*R*)- and (*S*)- enantiomer of 2-bromopentane ($\Delta_{R,S}\Delta G^\ddagger = \Delta_{R,S}\Delta H^\ddagger - T\Delta_{R,S}\Delta S^\ddagger$) and its enthalpic ($\Delta_{R,S}\Delta H^\ddagger$ ^{298 K}) and entropic ($T\Delta_{R,S}\Delta S^\ddagger$ ^{298 K}) terms. ^bData from Prokop et al.¹³

component of DbjA enantioselectivity are four times and seven times greater in absolute values, respectively, than DhaA.

For the decomposition of the SSF spectrum into its separate components, the excitation wavelength was set to 320 nm in order to predominantly excite the neutral form of the fluorophore. The neutral form then populates the complexed, anionic and tautomeric forms (Figure 1A). As shown in Figure 1C, the fluorescence emission of DhaA:C176UAA originates from the neutral, complexed and anionic forms. The tautomer contributes only marginally to the emission spectrum. Conversely, significant tautomer emission was observed for DbjA:G183UAA (Figure 1D). The formation of the tautomer in DbjA:G183UAA indicates that the chromophore is exposed to “structured water”, that is, water molecules with residence times longer than the fluorescence time scale. The presence of the tautomer was also confirmed by time-resolved fluorescence spectroscopy (Supporting Information Figure S4). The decay curve contained a negative component due to the population of the tautomer from the excited neutral species. Such particular feature of the fluorescence decay was not observed for DhaA:C176UAA. Because the tautomeric and anionic species are only formed in aqueous environments, their summed contributions to the overall signal reflect the hydration level within the dye’s microenvironment. The anionic and tautomeric forms account only for 50% of the emission signal of DhaA:C176UAA. However, 70% of the emission signal of DbjA:G183UAA can be attributed to these forms (Figure 1E, Supporting Information Table S4). This indicates that the microenvironment surrounding the UAA in DhaA:C176UAA is much less extensively hydrated than in DbjA:G183UAA. To further validate the approach, we thermally denatured the enzymes. The UAA originally buried within the protein interior becomes exposed to more hydrated microenvironment upon the denaturation process. As expected, for both enzymes the increasing temperature causes an increase in the contribution of the anion at the expense of the others forms, leading to the growth of $A^A + A^T$ parameter (Figure 1E, Supporting Information Table S4).

Replicated 200 ns MD simulations were performed for both labeled and wild type structures of studied enzymes. The periodic-boundary NPT simulations were carried out in AMBER12 (University of California, San Francisco, 2012) using ff10 force field (Supporting Information Table S5 and Figure S5).^{21–23} The level of hydration within the tunnel mouth of the wild type enzymes was about 1.7-times higher in DbjA than in DhaA (Table 2). The MD simulations show that the UAA is in one dominant conformation in the tunnel of DhaA:C176UAA (Supporting Information Figure S6). Conversely, the wider tunnel mouth of DbjA:G183UAA allowed the UAA to adopt two equally relevant stable conformations, one

Table 2. Hydration of Haloalkane Dehalogenases DhaA, DbjA, DhaA:C176UAA, and DbjA:G183UAA Revealed by Fluorescence Spectroscopy and Molecular Dynamics Simulations^b

parameter	DhaA:C176UAA	DbjA:G183UAA	DhaA	DbjA
overall contributions of anionic and tautomeric forms to the emission SSF spectra	UAA less hydrated	UAA more hydrated	less hydrated tunnel mouth ^a	more hydrated tunnel mouth ^a
<i>number of water molecules within 5 Å</i>	<i>9 ± 2</i>	<i>21 ± 5 or 28 ± 4</i>	<i>16 ± 4</i>	<i>27 ± 4</i>

^aThe enzymes have been characterized previously.¹¹ The methodology used was different from the SSF method. ^bExperimental parameters and results are presented in normal text; parameters and results obtained from MD simulations are presented in italics.

buried into the tunnel (UAA_3) and one more exposed (UAA_4; Supporting Information Table S6 and Figure S6). The simulations suggested that the UAA microenvironment is substantially less hydrated in DhaA:C176UAA than in both variants of DbjA:G183UAA (Table 2, Figure 2C), which is consistent with our experimental results. Additionally, the simulation indicated that the fluorophore often forms hydrogen bonds with adjacent amino acid residues, Thr148 in DhaA:C176UAA and Glu146 in DbjA:G183UAA, and with amino acids whose side chains contain amino groups, His272 for DhaA:C176UAA and Arg179 or His139 for DbjA:G183UAA (Figure 2B, Supporting Information Table S7). This may facilitate the formation of the complexed form detected in our experiments. Finally, the simulations indicated that water molecules in the microenvironment of the buried conformation of DbjA:G183UAA have residence times of up to 60 ns, which is much longer than the fluorescence time scale (Supporting Information Figure S7). This explains the strong contribution of the tautomeric form for this mutant. Such extremely long residence times are not found in structures without UAA (Supporting Information Figure S7). This suggests that the “structured water” detected in DbjA:G183UAA is induced by the UAA itself locking several water molecules within the active site pocket.

CONCLUSIONS

Recent findings emphasizing the importance of dynamics and hydration in enzymatic catalysis and rational protein design^{2,3} have created a strong demand for methods that provide site-specific information on these factors. In our approach, site-specificity is guaranteed by using UAA. SSF spectroscopic analysis of the hydroxycoumarin probe incorporated into the structure of the enzymes is a strikingly simple and universally applicable experimental procedure. The photophysics of the UAA provide qualitative information on the extent of hydration as demonstrated for two HLDs with already characterized hydration levels.¹¹ Although MD simulations show that incorporation of the chromophore can influence the residential times of water molecules, the conclusions on the hydration levels are valid. Given the ongoing development of UAA technology, this method could potentially be used to analyze hydration at specific sites in a wide range of proteins.

ASSOCIATED CONTENT

Supporting Information

Experimental procedures, synthesis of UAA, results of emission spectra deconvolution, CD spectra, and results from MD simulations. This material is available free of charge via the Internet at <http://pubs.acs.org>.

AUTHOR INFORMATION

Corresponding Authors

*paruch@chemi.muni.cz

*hof@jh-inst.cas.cz

*jiri@chemi.muni.cz

Present Address

#Great Lakes Bioenergy Research Center, College of Engineering, University of Wisconsin-Madison, Wisconsin 53706-1567, United States.

Notes

The authors declare no competing financial interest.

ACKNOWLEDGMENTS

Prof. Peter G. Schultz and Dr. Jeremy Mills from The Scripps Research Institute (USA) are greatly acknowledged for providing genetic material and valuable advices in UAA technology. Financial support from the Czech Science Foundation via grants P208/12/G016 (M.H. and J.S.) and P207/12/0775 (R.Ch.) and the Ministry of Education of the Czech Republic (LO1214; CZ.1.05/1.1.00/02.0123) is acknowledged. Moreover, M.H. acknowledges the Praemium Academie Award from Academy of Sciences of the Czech Republic. The work of J.B. and K.B. was supported by Program of “Employment of Best Young Scientists for International Cooperation Empowerment” (CZ1.07/2.3.00/30.0037) with cofinancing from the European Social Fund and the state budget of the Czech Republic. MetaCentrum is acknowledged for providing access to their computing facilities, supported by the Ministry of Education of the Czech Republic (LM2010005). CERIT-SC is acknowledged for providing access to their computing facilities, under the program Center CERIT scientific Cloud (CZ.1.05/3.2.00/08.0144).

REFERENCES

- (1) Fogarty, A. C.; Duboue-Dijon, E.; Sterpone, F.; Hynes, J. T.; Laage, D. *Chem. Soc. Rev.* **2013**, *42*, 5672.
- (2) Privett, H. K.; Kiss, G.; Lee, T. M.; Blomberg, R.; Chica, R. A.; Thomas, L. M.; Hilvert, D.; Houk, K. N.; Mayo, S. L. *Proc. Natl. Acad. Sci. U. S. A.* **2012**, *109*, 3790.
- (3) Sykora, J.; Brezovsky, J.; Koudelakova, T.; Lahoda, M.; Fortova, A.; Chernovets, T.; Chaloupkova, R.; Stepankova, V.; Prokop, Z.; Kuta Smatanova, L.; Hof, M.; Damborsky, J. *Nat. Chem. Biol.* **2014**, *10*, 428.
- (4) Sekhar, A.; Vallurupalli, P.; Kay, L. E. *Proc. Natl. Acad. Sci. U. S. A.* **2013**, *110*, 11391.
- (5) Levy, Y.; Onuchic, J. N. *Annu. Rev. Biophys. Biomol. Struct.* **2006**, *35*, 389.
- (6) Grossman, M.; Born, B.; Heyden, M.; Tworowski, D.; Fields, G. B.; Sagi, I.; Havenith, M. *Nat. Struct. Mol. Biol.* **2011**, *18*, 1102.
- (7) Nucci, N. V.; Pometun, M. S.; Wand, A. J. *Nat. Struct. Mol. Biol.* **2011**, *18*, 245.
- (8) Russo, D.; Hura, G.; Head-Gordon, T. *Biophys. J.* **2004**, *86*, 1852.
- (9) Oleinikova, A.; Sasisanker, P.; Weingartner, H. *J. Phys. Chem. B* **2004**, *108*, 8467.
- (10) King, J. T.; Kubarych, K. J. *J. Am. Chem. Soc.* **2012**, *134*, 18705.
- (11) Jesenska, A.; Sykora, J.; Olzyska, A.; Brezovsky, J.; Zdrahal, Z.; Damborsky, J.; Hof, M. *J. Am. Chem. Soc.* **2009**, *131*, 494.
- (12) Summerer, D.; Chen, S.; Wu, N.; Deiters, A.; Chin, J. W.; Schultz, P. G. *Proc. Natl. Acad. Sci. U. S. A.* **2006**, *103*, 9785.

- (13) Prokop, Z.; Sato, Y.; Brezovsky, J.; Mozga, T.; Chaloupkova, R.; Koudelakova, T.; Jerabek, P.; Stepankova, V.; Natsume, R.; van Leeuwen, J. G. E.; Janssen, D. B.; Florian, J.; Nagata, Y.; Senda, T.; Damborsky, J. *Angew. Chem., Int. Ed.* **2010**, *49*, 6111.
- (14) Schultz, P. G.; Mills, J. H.; Lee, H. S.; Liu, C. C.; Wang, J. Y. *ChemBioChem.* **2009**, *10*, 2162.
- (15) Choudhury, S. D.; Nath, S.; Pal, H. *J. Phys. Chem. B* **2008**, *112*, 7748.
- (16) Choudhury, S. D.; Pal, H. *J. Phys. Chem. B* **2009**, *113*, 6736.
- (17) Moriya, T. *Bull. Chem. Soc. Jpn.* **1983**, *56*, 6.
- (18) Wang, J. Y.; Xie, J. M.; Schultz, P. G. *J. Am. Chem. Soc.* **2006**, *128*, 8738.
- (19) Kulakova, A. N.; Larkin, M. J.; Kulakov, L. A. *Microbiology* **1997**, *143*, 109.
- (20) Sato, Y.; Monincova, M.; Chaloupkova, R.; Prokop, Z.; Ohtsubo, Y.; Minamisawa, K.; Tsuda, M.; Damborsky, J.; Nagata, Y. *Appl. Environ. Microb.* **2005**, *71*, 4372.
- (21) Hornak, V.; Abel, R.; Okur, A.; Strockbine, B.; Roitberg, A.; Simmerling, C. *Proteins* **2006**, *65*, 712.
- (22) Joung, I. S.; Cheatham, T. E. *J. Phys. Chem. B* **2008**, *112*, 9020.
- (23) Joung, I. S.; Cheatham, T. E. *J. Phys. Chem. B* **2009**, *113*, 13279.